Highspeed laser welding of steel using a high-power single-mode continuous-wave fiber laser

J. Drechsel, U. Loeschner, S. Schwind, L. Hartwig, J. Schille, H. Exner, P. Huebner, A. Eysert

Laser Institute at the University of Applied Sciences, Technikumplatz 17, Mittweida, Germany

ABSTRACT

Since a few years, high brilliance laser sources find their way into laser material processing. Laser micro processing by applying high brilliance laser radiation up to 3 kW of continuous wave laser power in combination with ultrafast beam deflection systems has been successfully demonstrated in 2008 for the first time. In the fields of laser welding, high brilliant laser radiation was mainly used for micro welding, but up to now the macro range is still insufficiently investigated.

Hence, this study reports on detailed investigations of high speed laser welding of different steel grades, performed with a high power single mode fiber laser source. The laser beam was deflected relative to the sample by using both a fast galvanometer scanner system with f-theta focusing objective and a linear axis in combination with a welding optic, respectively. In the study, the mainly process influencing parameters such as laser power, welding speed, thickness of the metal sheets, angle of incidence and laser beam spot size were varied in a wide range. The weld seam quality was evaluated by structural analyses, static tensile tests and EDX measurements. Finally, the laser welding process has been optimized for different weld seam geometries, for example bead-on-plate welds and butt welds.

Keywords: laser welding, fiber laser welding, highspeed laser welding

1. INTRODUCTION

Welding using high-brilliant laser radiation has been widely investigated in the micro scale range. Based on the results presented in [1] in this paper this technique will be transferred to high-speed welding in the macro range. As known, laser beam deep penetration welding requires intensities of more than 10^6 W/cm^2. In deep penetration welding, the material will be melted and partially vaporized leading to a keyhole in the center of the weld pool. By multiple reflections at the capillary wall laser radiation penetrates in deeper material regions and will be more strongly absorbed. Thereby, high process efficiency and fast welding speeds can be achieved resulting in slim weld seams with a penetration depth of more than 15 mm. As reported in [2], high intensity of laser radiation is beneficial for the welding process. High power single mode fiber laser sources can provide high laser power of several kilowatts and excellent beam quality and thus intensities of laser radiation up to 10^9 W/cm² can be achieved. As a result, the mainly limiting factors of solid state laser sources in laser welding are eliminated.

In laser welding two principles are established for relative movement between the laser beam and the sample surface. In remote laser welding the laser beam deflection across the sample surface is realized via scan systems [3]. On the other hand, either the sample or the welding optic will be moved by an axis system or a robot. The two laser beam deflection principles are qualified for highspeed laser welding with welding speeds of up to 100 m/min, but remote welding with scanner offers higher degree of dynamic.

As reported in numerous investigations of the laser welding process, such as [4,5], the humping effect reduces the quality of weld joints especially when high welding speeds are applied. Humping describes periodically arranged humps along the weld seam occurring outside the current position of the laser beam at the end of the weld pool due to the periodic fluctuation of the melt. The narrow keyhole is characterized by a large surface tension preventing further refilling from rear regions of the weld pool. The molten material will be accumulated in a droplet shape and solidified at the end of the weld pool due to the high welding speed and a large thermal gradient [5,6]. In addition, the inconstant density of the plasma supports humping formation. In a dense plasma laser radiation will be absorbed very well and thus, less laser power will impinge at sample surface. Therefore, less material is vaporized causing a lower plasma density that in turn

results in reduced absorption of laser radiation within the plasma plume accompanied by increased penetration depths. But, increased laser power, higher welding speed, and smaller spot size are beneficial for occurrence of humping [7].

Welding speed can be increased with the same ratio as the spot size is reduced without a loss in weld seam quality [8]. For example, with a spot size of 24 µm a welding speed of 100 m/min was achieved with an aspect ratio > 1:15 [9,10]. But, weld seam quality is constricted due to a gradually increase of the notching effect and formation of humping.

However, spiking is indicated as another phenomenon in laser welding describing a discontinuous formation of the welding root, and the material is only partially welded-through. Therefore it was pointed out, that the spiking effect is determined as a function of applied laser beam peak intensity and chosen laser power [11]. The occurrence of spiking depends on the position of the laser beam focal plane with respect to parabolic formed bottom of the keyhole [12]. Moreover, as a result of relative movement between laser focal plane and capillary bottom, changed conditions for reflection and absorption of laser radiation at the walls and at the bottom of the capillary lead to increased periodic melt formation. Thus, weld depth varies along the welding seam referred to as spiking.

2. EXPERIMENTAL DETAILS

The investigations were performed with a continuous-wave single-mode fiber laser, which emits at a central wavelength of 1070 nm and delivers a maximum laser power of 3 kW.

In addition, the machining facility is equipped with a galvanometer scan system from Raylase AG and alternatively with a welding head from Precitec KG for laser beam focusing. For the scanner system two f-theta objectives with focal lengths of 230 mm and 500 mm were available, whereas the focal length of the welding optic was 250 mm. The corresponding focal spot sizes on the material surface were estimated by means of a beam diagnostic system from PRIMES using the 86%-method.

There are two principles realizing a relative movement between laser beam and sample surface: laser beam deflection onto the sample by scanner or moving the sample with an axis system while the stationary laser beam is focused by the welding optic. Using the galvanometer scanner for beam deflection, the varying angle of incidence onto the material during movement has to be considered. By restricting the beam movement to the center region of the scan field, this influence can be neglected. Significant parameters of the laser machining system are summarized in table 1.

Table 1: Significant parameters of the laser system.

focussing system	**galvanometer scanner**		**welding head**
laser power on sample surface [kW]	2.5		1.84
focal length [mm]	230	500	250
focal spot size d_{86} [µm]	21	65	53
maximum speed [m/min]	1200	2580	135
peak intensity with TEM_{00} [W/cm²]	$14.4 \cdot 10^8$	$1.5 \cdot 10^8$	$1.6 \cdot 10^8$

Experiments performed with the welding head in combination with axis movement allow static angles of incidence during movement. Accordingly, the influence of predefined inclined laser beams impinging on the sample surface was investigated in greater detail by tilting the welding head relative to the sample surface. Tilting the welding head in welding direction is called backhand welding and, towards the welding direction means forehand welding.

Figure 1 depicts details of the experimental setup. In the photograph in the experimental arrangement with the tilted welding head is shown.

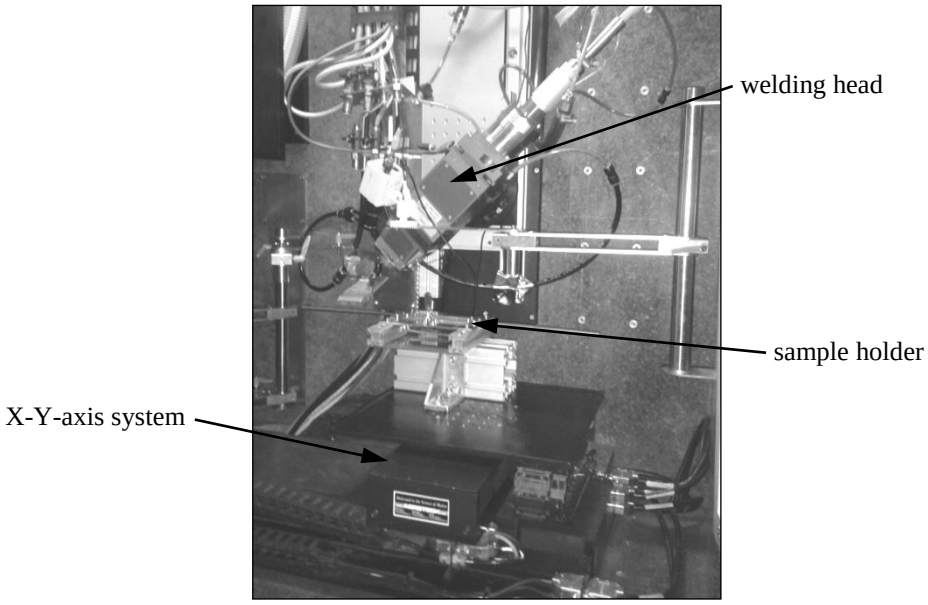

Figure 1: Experimental setup: tilted welding head, X-Y-axis system, sample holder.

Welding investigations were conducted with two different steel grades: stainless steel SS 304 and a cold-rolled steel 22MnB5. The SS304 is a corrosion-resistant and acid-proof, high-alloy, fully austenitic stainless steel. It has a tensile strength of about 640 MPa. Sheet thickness ranges between 1 and 3 mm. The austenitic structure of SS304 is preserved after welding.

The 22MnB5 is a manganese- and boron-alloyed, fully martensitic quenched and tempered steel grade with a zinc surface coating. It has a tensile strength of 1500 MPa. In figure 2 a cross-section of 22MnB5 is presented. The thickness of the zinc layer was of about 20 µm, while the sheet thickness amounts to 1.6 mm. In general, welding of this steel material using conventional welding techniques is commonly avoided because of a substantial loss of hardness in the heat affected zone resulting in a reduced strength.

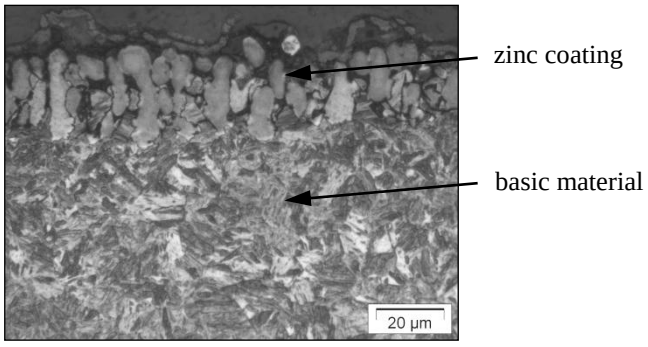

Figure 2: Cross-section photograph of 22MnB5: 20 µm thick zinc coating on the steel surface is clearly visible.

In the investigations the influence of important process parameters such as applied laser power, welding speed, beam spot size, material thickness, and the angle of incidence of the laser radiation on the welding result was determined for both materials. All experiments were performed with the premise of weld through the respective material thickness. Besides, no shielding gas was used.

First, bead-on-plate weld tests were done using the galvanometer scanner and varying laser power, welding speed, and laser spot size in order to find suitable parameters for the highspeed laser welding process. Thereby, the limits for the welding process are given by humping and spiking. Afterwards, bead-on-plate welding tests were performed by using the welding head in combination with the axis system. This setup allows detailed investigations on the influence of a varied angle of incidence on the welding process.

Based on previous investigations butt welds were generated with optimum parameters. Due to the very low laser spot sizes provided by excellent laser beam quality and therefore expected weld widths in the order of only 0.1 mm additional edge preparation was required. Therefore, laser cut edges were aftertreated by a grinding process to guarantee a joint gap less than 30 µm.

Weld seams were characterized by optical microscopy analyses. By means of cross section polish preparation the geometrical parameters weld width and seam shape were determined. In addition, tensile tests were performed to assess the tensile strength of welded samples in comparison to the basic material.

3. RESULTS AND DISCUSSION

3.1 Bead-on-plate weld results

In first investigations the respective maximum welding speed was determined when laser power was increased, starting at a laser power level of 920 W. As mentioned above in all experiments the samples were completely welded through and showed a continuous root formation at the bottom. In figure 3 the welding speed as a function of laser power and material thickness for both materials is presented. Generally, with rising laser power the scan speed increases, but at a distinct high laser power level the course become degressive except of the 22MnB5. That means a further increase of laser power lead to a progressively slight growth of the welding speed.

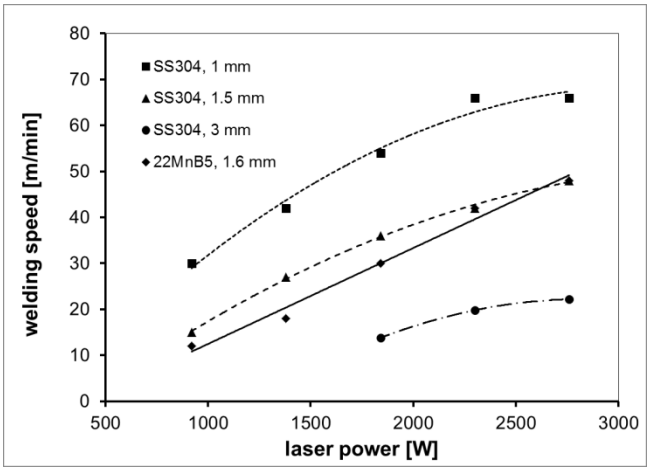

Figure 3: Maximum welding speed for SS304 and 22MnB5 as a function of laser power for bead-on-plate welds with different sheet thicknesses, parameter: d_{86} = 65 µm.

At a given laser power the highest welding speed was achieved with the lowest sheet thickness of 1 mm. For instance, if a laser power of 2.3 kW was applied, the welding speed is 66 m/min. For a sheet thickness of 3 mm the welding speed is reduced to 20 m/min. But, the limiting effects of humping and spiking are not considered in figure 3. Humping appears gradually when the process parameters are changed. There is a transition from typical weld reinforcement to hump formation induced by increasing welding speed, shown in figure 4a)-c). At the beginning, single irregular shaped humps are generated, followed by periodic hump formation at raised welding speed. Also, spiking was observed at the bottom of the weld seam when process parameters are changed, see figure 5a)-c). The spiking effect leads to discontinuous root formation. Thus, weld depth varied along the seam and the material was only partially welded through.

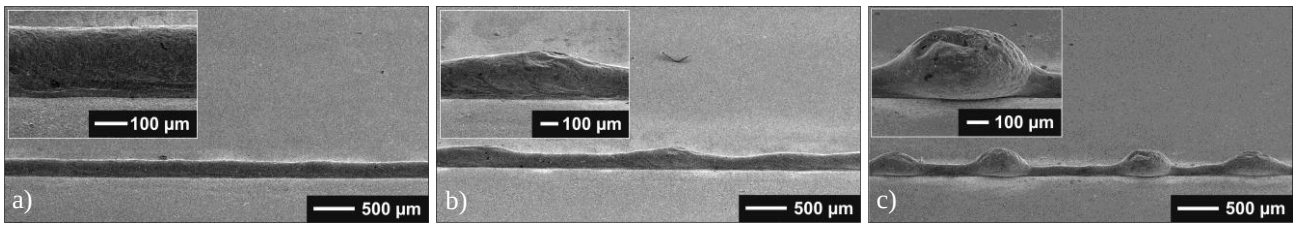

Figure 4: Humping formation for SS304 weld seams, parameters: P_{cw} = 1380 W; sheet thickness1.5 mm; a) homogeneous humping-free seam, v = 24 m/min; b) incipient humping, v = 27 m/min; c) humping, v = 36 m/min.

It was found that with a minimum spot size of 21 µm humping occurs over the whole range of investigated parameters. Applying a larger spot size of 65 µm humping occurs above a sheet thickness dependent laser power level. For a 1 mm thick sheet of SS 304 a laser power limit of 920 W and for a thickness of 1.5 mm a maximum laser power of 1380 W were determined. In figure 6 the occurrence of humping as a function of welding speed and material thickness for a given laser spot size of 65 µm is shown. There exists a transition zone between humping-free and humping-affected weld re-

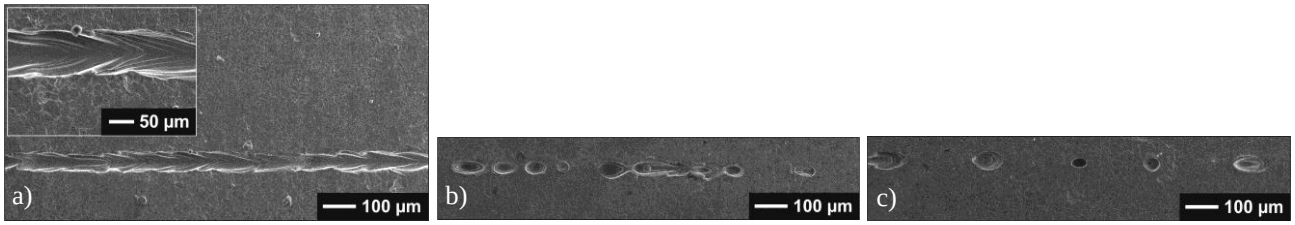

Figure 5: Spiking formation on SS304 weld roots, parameters: P_{cw} = 1380 W; sheet thickness 1.5 mm; a) homogeneously formed root, v = 27 m/min; b) non-uniform root formation indicates incipient spiking; v = 30 m/min; c) spiking, v = 33 m/min).

sults of SS304 for all investigated material thicknesses when welding speed increases. So in conclusion, welding speed is reduced for humping-free weld seams. Due to higher thermal conductivity of 22MnB5 the melting behaviour, which considerably influences the humping effect, is quite different. Therefore 22MnB5 shows a stronger humping tendency in comparison to SS304 resulting in a less maximum welding speed for humping-free weld seams.

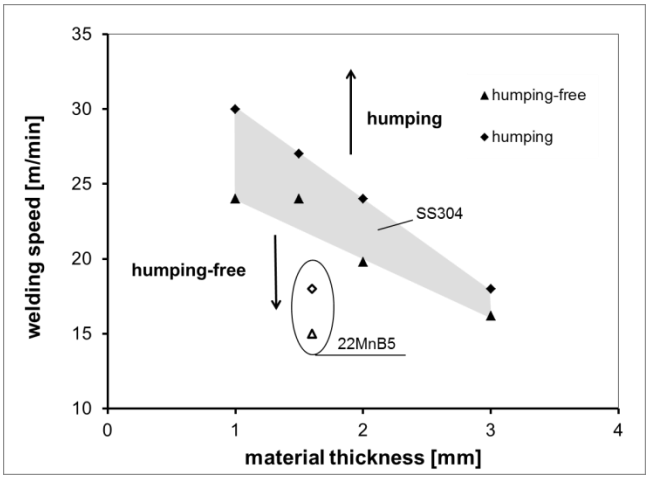

Figure 6: Maximum welding speed as a function of sheet thicknesses for SS304 and 22MnB5 for bead-on-plate welds, parameter: d_{86} = 65 µm.

The seams of all welded specimens show a nail-shaped cross section, as demonstrated in figure 7b). The microstructure within the welding seam is almost homogeneous for both studied materials. Grain size and shape are quite similar in comparison to the basic material.

The welding bead width depends on applied process parameter sets, as can be seen in figure 7a). For a given laser power the welding bead width is sinking when welding speed is increased. This is in accordance to the reduced energy input per unit length, defined as the ratio of applied laser power and welding speed. With rising laser power this effect is less pronounced. But, for a certain welding speed the seam width was much larger when higher level of laser power was applied. Increased laser power means a larger laser beam diameter, which overcome the intensity threshold for melting resulting in a wider welding bead. Within the investigated parameters according to figure 7, welding bead width ranges between 190 µm and 265 µm.

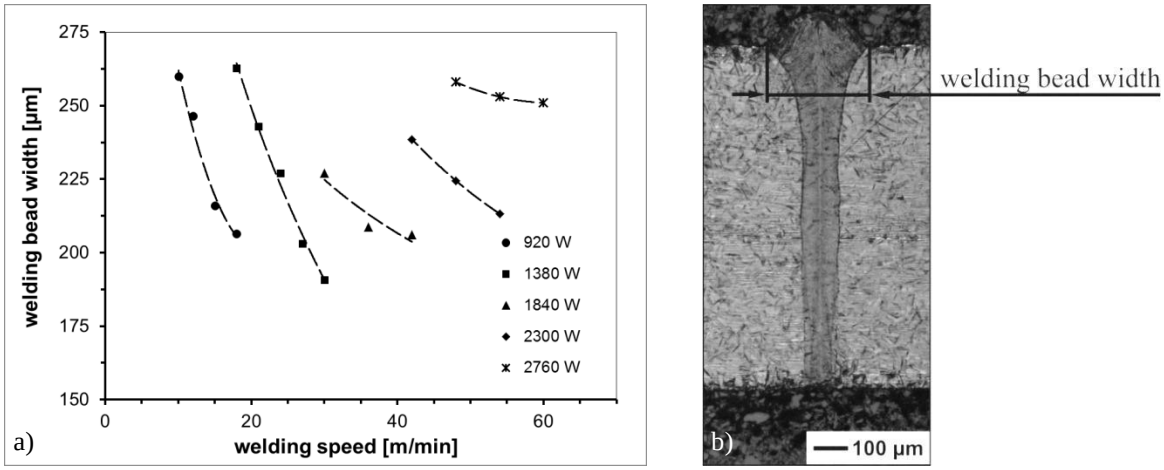

Figure 7: a) welding bead width as a function of welding speed and laser power, parameters: SS304, sheet thickness 1.5 mm; b) cross section photograph of a typical weld seam with nail-shaped head, parameters: P_{cw} = 920 W, v = 18 m/min, d_{86} = 65 µm; SS304; sheet thickness 1mm.

3.2 Influence of the angle of incidence on the welding process

Plasma formation is almost present in deep penetration welding. As discussed above, dense plasma adversely influences the laser welding process with respect to humping-free weld seams at high welding speed. There is a simple method to reduce the plasma impact during the welding process: forehand welding and backhand welding can be realized by changing the angle of incident laser radiation which reduces plasma interaction with incident laser radiation. Inclined laser beams with respect to the sample surface were accomplished by tilting the welding head.

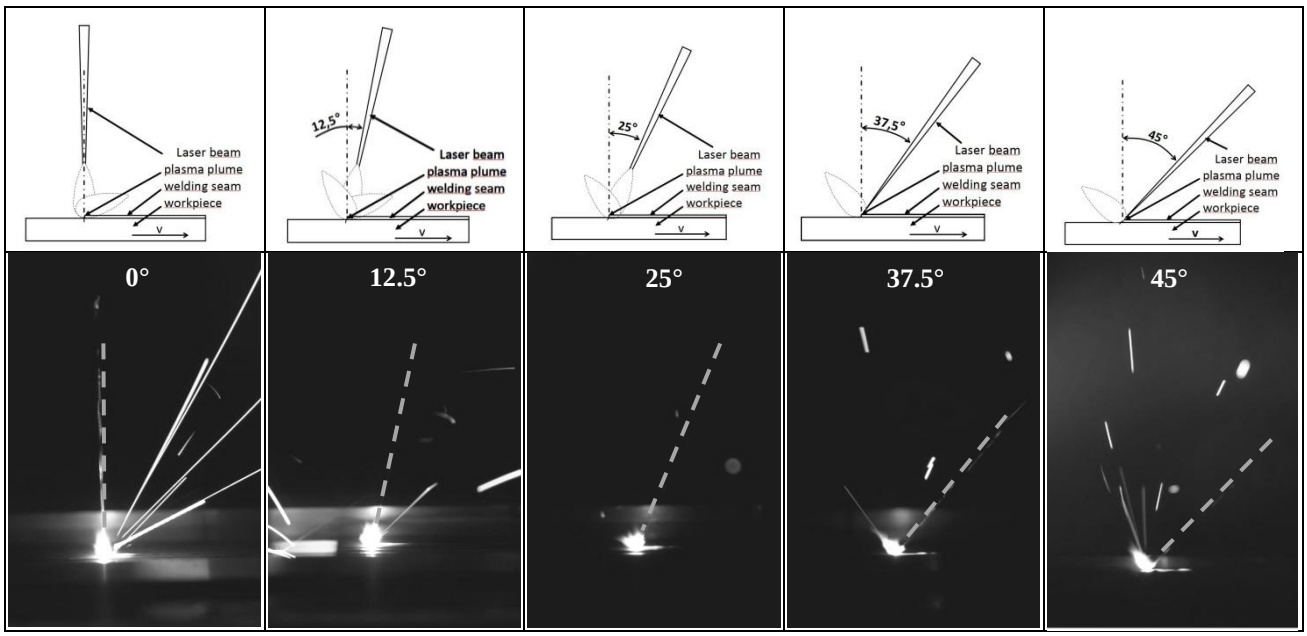

Figure 8: upper row) schematic drawings illustrating the angle of the incident laser beam and the preferred orientation of the plasma plume during welding, lower row) photographs of plasma plume formation during welding (dashed line: direction of incident laser beam), parameters: P_{cw} = 1.84 kW, v = 18 m/min, d_{86} = 53 µm, SS304.

Backhand welding investigations have been not beneficial for lowering the humping threshold. However, the humping threshold can be shifted to higher welding speeds using forehand welding. In figure 8 welding conditions as well as photographs of observed variations in the orientation of the plasma plume during the welding process are demonstrated in

detail. Schematic drawings in the upper row in figure 8 illustrate the angle of incidence of the laser beam and the preferred orientation of the plasma plume. In the photographs the incident laser beam is marked with a red line. Up to an angle of 25° the orientation of plasma plume varied relative to the direction of the incident laser beam without a preferred orientation. A further increase of the angle lead to preferred orientation of the plasma plume in the opposite direction related to the incident laser beam. If the angle of incidence is above 45° the material cannot be weld through anymore.

The maximum welding speed for the generation of humping-free welds as a function of the applied laser power and the angle of incidence for a given sheet thickness of 2 mm is shown in figure 9. In principle, using forehand welding a considerably higher welding speed was achieved with increased inclination of the laser beam. But, for a given sheet thickness the laser power has to be adapted according to the increase of inclination because of a rising nominal material thickness to be weld through. In comparison to the results presented in figure 6 the maximum welding speed achieved with the welding head is much lower for a sheet thickness of 2 mm. This effect is attributed to a significant smaller spot size of 53 µm delivered by the welding optic, which results in a 50% higher intensity of laser radiation. Hence, humping threshold is lowered.

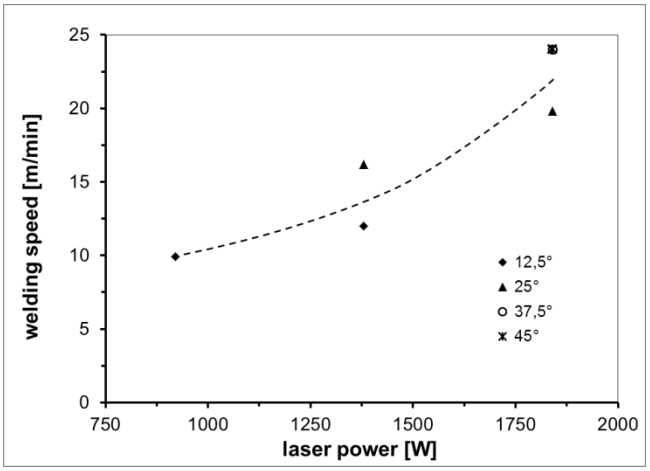

Figure 9: Maximum welding speed allowing humping- free weld seams as a function of the angle of incidence and laser power, parameters: d_{86} = 53 µm, sheet thickness 2mm, SS304.

3.3 Butt welding results

Based on optimized bead-on-plate weld results butt welds were generated by using the welding head, which was tilted by an angle of 45° with respect to the sample surface. In figure 10 maximum achieved welding speeds are shown as a function of material thick-ness realized with bead-on-plate welds as well as butt welds for SS304 and 22MnB5. For SS304 the welding speed can be considerably increased when forehand welding with an inclined laser beam is performed. For example, welding speed rises from 24 m/min up to 48 m/min for a 1 mm thick bead-on-plate welded sheet, when the tilt angle is set to 45°. For butt welds comparable welding speeds were obtained. However, for thicker sheets the effect becomes gradually smaller and only amounts to 20% for a material thickness of 2 mm. Having a look at 22 MnB5, the benefit of welding speed is slightly less in comparison to SS304 at a comparable sheet thickness.

Despite of the high demands on the lateral positioning accuracy to achieve a joint gap smaller than 30 µm butt welds can be generated reproducibly with both materials. A typical weld seam for SS304 is shown in figure 11a), characterized by a narrow weld seam width of 150 µm and a welding bead width of approximately 330 µm. For a given welding depth of 2 mm it corresponds to an aspect ratio of 1:13.

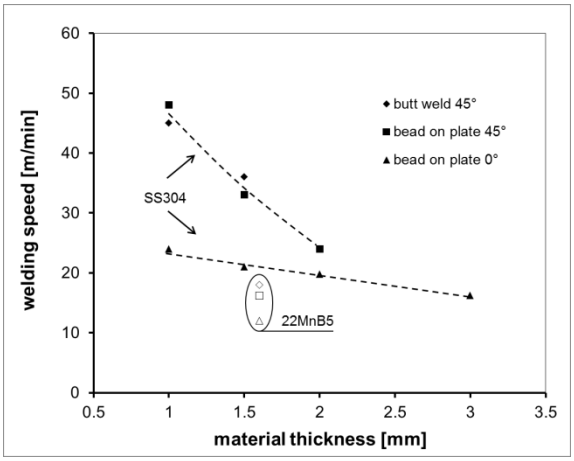

Figure 10: Welding speed as a function of material thickness depending on material and angle of incidence for bead-on-plate welds and butt welds, parameter: d_{86} = 53 µm.

Hardness profiles within the heat affected zone give information on the strength and the brittleness of the weld joint. A hardness increase as well as a large gradient of the hardness profile within the heat affected zone is disadvantageous with respect to with respect to weld strength. The hardness profile of the welds was measured at cross section polishes. For SS304 a slight hardness increase of 20% corresponding to 240 HV [0.1] in comparison to the initial hardness of the basic material of 200 HV [0.1] was measured in a region of +/- 100 µm around the center of weld seam, see figure 11. In a wider region of +/-300 µm a slight increase in hardness of approximately 10% according to 220 HV [0.2] was determined, caused by heat effects.

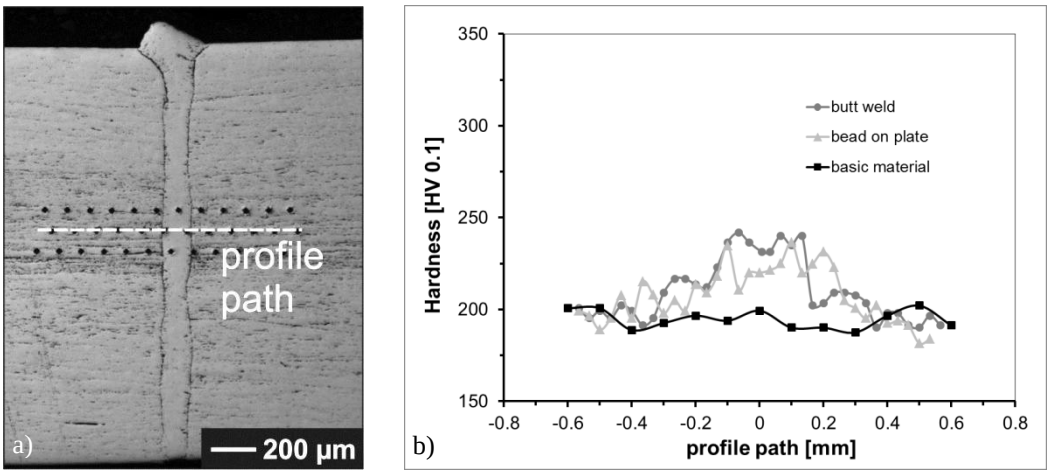

Figure 11: a) cross-section photograph of a butt weld, parameters: P_{cw} = 1840 W; v = 18 m/min; d_{86} = 53 µm; SS304; b) corresponding hardness profile.

However, for 22MnB5 the hardness profile is quite different in comparison to SS304, as can be seen in figure 12. Inwards the 250 µm wide weld seam an increase in hardness of 20% corresponding to 600 HV [0.2] was measured, compared to 500 HV [0.2] for the basic material. But, within the heat affected zone next to the weld seam a considerable drop of hardness of 25% down to 370 HV [0.2] was observed. The initial hardness of the basic material was achieved in a distance of +/-350 µm away from weld seam center.

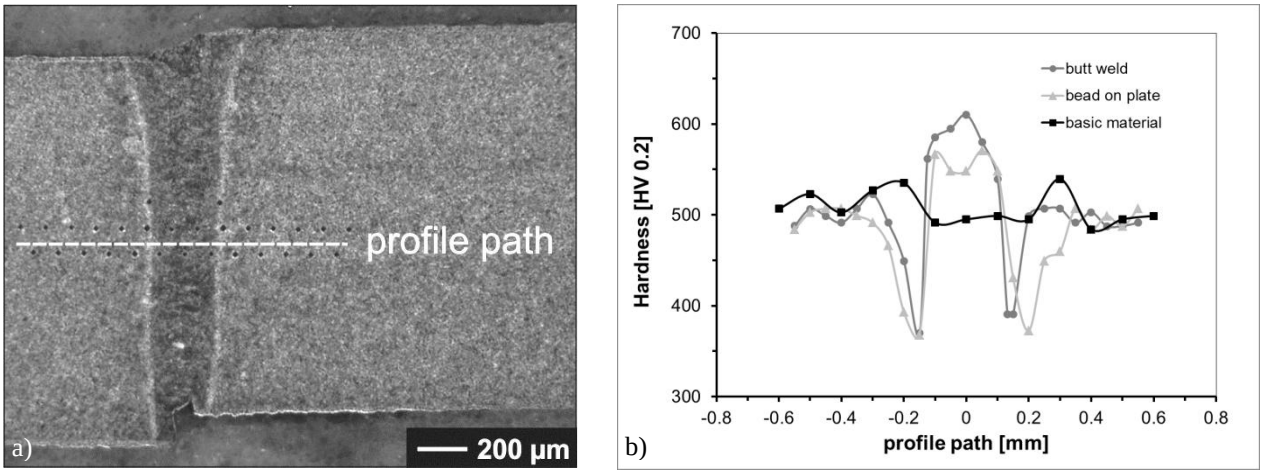

Figure 12: a) cross-section photograph of a butt weld, parameters: P_{cw} = 1840 W; v = 16 m/min; d_{86} = 53 µm; 22MnB5; b) corresponding hardness profile.

3.4 Tensile test results

Tensile tests were performed with butt-welded samples, bead-on-plate welded samples as well as basic material samples of SS304 and 22MnB5 with a thickness of 1.5 mm and 1.6 mm, respectively. For SS304 a typical large strain zone is present in the stress-strain-curve, demonstrated in figure 13. All samples show the same maximum tensile strength of 650 MPa before they tear. Comparing the maximum tensile strength of welded samples and basic material, there is no change which confirms the good weldability.

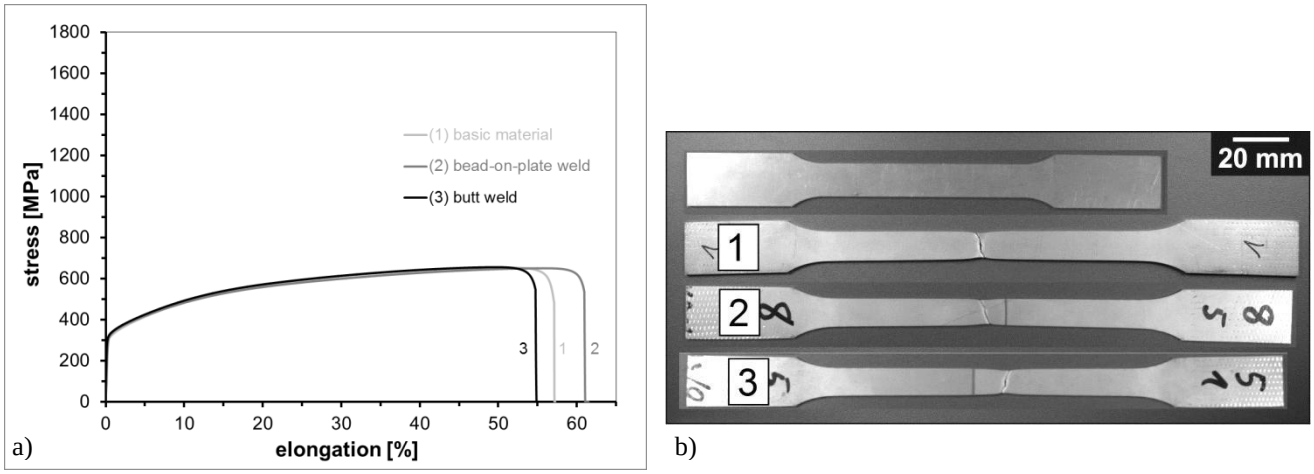

Figure 13: Tensile test results performed with SS304 samples, a) stress-strain-curve, b) samples: (1) basic material, (2) bead-on-plate weld, (3) butt weld.

Tensile test of 22MnB5 reveal a very low tensile elongation, shown in figure 14. Butt weld seams as well as bead-on-plate welds tear almost exclusively in the vicinity of the weld seam in the heat affected zone. But, the loss of tensile strength is only 10% in comparison to the basic material. This is in contrast to results obtained with conventional welding techniques. Because of a significant smaller heat affected zone in laser welding, the hardened weld seam acts as a stiff element that reduces the notching effect of less strength material arranged in the narrow heat affected zone.

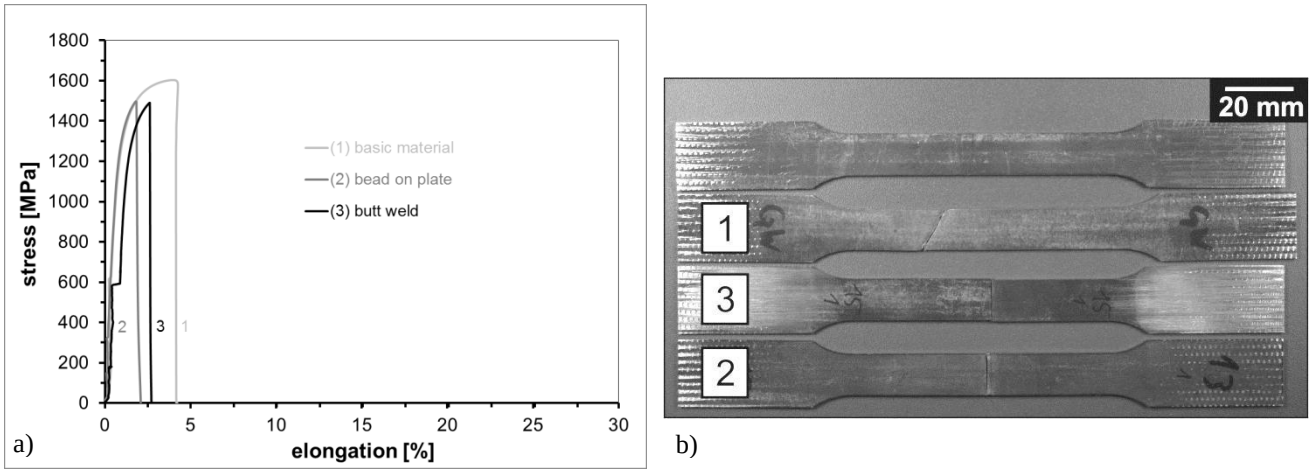

Figure 14: Tensile test results performed with 22MnB5 samples; a) stress-strain-curve; b) samples: (1) basic material, (2) bead-on-plate weld, (3) butt weld.

4. CONCLUSIONS

In this paper highspeed welding of steel using a brilliant high power fiber laser with a maximum laser output power of 3 kW is presented.

It has been found that the maximum welding speed is limited by humping. The humping effect strongly depends on applied parameters, such as laser power, spot size, and welding speed. Thus, for humping-free weld seams applicable process parameters are constricted. In addition, the maximum welding speed is reduced for thicker sheets. For example a 1 mm thick sheet of SS304 was welded with a welding speed of 24 m/min and a 3 mm thick sample with 16 m/min, respectively. The 22 MnB5 shows a stronger humping tendency resulting in lower usable welding speed of 15 m/min for a sheet thickness of 1.6 mm.

By implementing forehand welding realized by tilting the welding head the welding speed increased up to 45 m/min for a 1 mm thick butt welded sheet of SS304 without humping. For 22 MnB5 an increase in welding speed by a factor of 1.5 was achieved in comparison to values obtained with vertical incidence of laser radiation.

Performing highspeed laser welding using a brilliant laser source narrow weld seams were generated, characterized by a high degree of mechanical strength. In particular, 22MnB5 samples were butt welded with a loss of tensile strength of only 10%, although the material is classified as difficult to weld with conventional welding technologies.

However, due to excellent beam quality and therefore small laser spot sizes of only several tens of micrometer a joint gap in the order of only 30 µm is tolerable. Thus, additional seam preparation of laser cut edges by a grinding process was required.

ACKNOWLEDGMENT

The authors gratefully acknowledge financial support of the presented work by the Federal Ministry of Education and Research (project number 03IPT506X).

REFERENCES

[1] Hartwig, L., Ebert, R., Kloetzer, S., Weinhold, S., Drechsel, J., Peukert, F., Schille, J., Exner, H., “Material pro-cessing with a 3 kW single mode fibre laser.” JLMN-Journal of LaserMicro/Nanoengeneering, Vol. 5 No. 2, 128-133 (2010).

[2] Weberpals, J.P., “Nutzen und Grenzen guter Fokussierbarkeit beim Laserschweissen,” German dissertation, Stuttgart University, ISBN 978-3-8316-0995-6 (2010).

[3] Klotzbach, A., Hartmann, A., Morgenthal, L., “Laserstrahlschweißen im kW-Leistungsbereich durch schnelle Strahlablenkung,” Proc. 13. International Scientific Konferenz Mittweida, Journal of the Mittweida University of Technology and Economics, No. 9 Lasertechnik, 149-156 (1998).

[4] Berger, P., Huegel, H., Hess, A., Weber, R. and Graf, T., “Understanding of Humping Based on Conservation of Volume Flow,” Physics Procedia 12, 232-240 (2011).

[5] Wei, P. S., Chuang, K.C., Ku, J.S., DebRoy, T., “Mechanisms of Spiking and Humping in Keyhole welding,” IEEE transactions on components, packaging and manufacturing technology, Vol. 2, No. 3, 383-394 (2012).

[6] Kawahito, Y., Mizutani, M., Katayama, S., “Investigation of High Power Fiber Laser Welding Phenomena of Stainless Steel,” Transactions of Joining and Welding Research Institute, Osaka University, Vol. 36 No. 2, 11-15 (2007).

[7] Kittel, S., “Welding with brilliant lasers - prospects and limitations for industrial applications,” 4th Workshop on Fiber Lasers, November 5-6, Dresden, Germany (2008).

[8] Kittel, S., Dausinger, F., “Welding with Brilliant Lasers: Prospects and Limitations,” Proc. SPIE 7585, 758502 (2010).

[9] Berger, P., “Modellierung des Laserstrahlschweissens - Ein Weg zum Prozessverstaendnis,” Laser Technik Journal April No.2, 31-34. (2007).

[10] Armstrong, R.E., “Control of spiking in partial penetration electron beam welds,” Welding Journal, Vol. 49 No. 8, 382-388 (1970).

[11] Wei, P.S., Ho, C.Y., “Beam focusing characteristics effect on energy reflection and absorption in a drilling or welding cavity of paraboloid of revolution,” Int. Journal Heat Mass Transf., Vol. 41 No. 21, 3299–3308 (1998).

[12] Neumann, S., Seefeld, T. “Humping in single mode laser beam welding of different materials,” Proc. of the Fifth Int. WLT-Conference on Lasers in Manufacturing 2009, 9-14 (2009).